HEFAT2014
10th International Conference on Heat Transfer, Fluid Mechanics and Thermodynamics
14–16 July 2014
Orlando, Florida

THERMODYNAMIC ANALYSIS FOR AN INCLINED CHANNEL CONTAINING TWO IMMISCIBLE COUPLE STRESS FLUIDS USING HAM

Ramana Murthy J V and Srinivas J*
*Author for correspondence
Department of Mathematics,
National Institute of Technology, Warangal, 506004, India,
E-mail: j.srinivasnit@gmail.com, jsrinivas@nitw.ac.in

ABSTRACT

In this paper, the flow of two immiscible couple stress fluids between two inclined parallel plates of a channel with constant wall temperatures is studied in terms of entropy generation rate. The flow is assumed to be governed by Stokes's couple stress fluid flow equation. The flow region consists of two zones, the flow of the heavier fluid taking place in the lower zone. The governing non-linear differential equations are then solved using Homotopy Analysis Method (HAM). Profiles of dimensionless velocity, temperature, entropy generation number and Bejan number are shown graphically for various values of couple stress parameter, Brinkman number, Grashof number, Reynolds number and viscous dissipation parameter. It is observed that couple stress fluid decreases the frictional forces and hence increases exergy.

INTRODUCTION

Entropy Generation Minimization Method: In the past few decades, it was observed that the first law of thermodynamics would not be capable of providing a clear insight into engine operations. For this reason, the use of the second law of thermodynamics has been intensified in internal combustion engines. The analysis of a process or a system with the second law of thermodynamics is termed availability or exergy analysis. The application of exergy analysis in engineering systems is very useful because it provides quantitative information about irreversibility and exergy losses in the system. In this way, the thermodynamic efficiency can be quantified and poor efficiency areas be identified, so that systems can be designed and operated more efficiently.

The thermodynamic irreversibility in any fluid flow process can be quantified through entropy analysis. The first law of thermodynamics is simply an expression of conservation of energy principle. The second law of thermodynamics states that all real processes are irreversible. Entropy generation is a measure of the account of irreversibility associated with the real processes. As entropy generation takes place, the quality of energy (i.e. exergy) decreases. In order to preserve the quality of energy in a fluid flow process or at least to reduce the entropy generation, it is important to study the distribution of the entropy generation within the fluid volume. The optimal design for any thermal system can be achieved by minimizing entropy generation in the system. Entropy generation in thermal engineering system destroys available work and thus reduces its efficiency. Many studies have been published to assess the sources of irreversibility in components and systems. This was first studied by Bejan [1, 2] and he gave good engineering sense for the study by focusing on irreversibility. This new concept is based on simultaneous application of first and second laws of thermodynamics in analysis and design of the systems. In the paper [1], he studied the heat transfer problems in the pipe flow, boundary layer flow past a plate, and flow in the entrance region of a rectangular duct using Entropy Generation Minimization (EGM) method and also explained various reasons behind entropy generation in applied thermal engineering where the generation of entropy destroys the available work, called exergy, of a system. Also Bejan [3] studied the entropy generation for forced convective heat transfer due to temperature gradient and viscosity effect in a fluid. Later on, many investigations have been carried to determine the entropy generation and Bejan profiles for different geometric arrangements, flow situations, and thermal boundary conditions. Several works on entropy generation minimization have appeared in the open literature [4]-[8].

Immiscible Fluids: The flow and heat transfer of immiscible fluids in inclined channel are of special importance in the petroleum extraction and transport problem. The reservoir rock of oil field contains many immiscible fluids in its pores. A portion of the pores contains water and the rest contains oil or gases or both. The immiscible flows in crude oil transport were studied experimentally by Bakhtiyarov and Siginer [9]. Malashetty and Umavathi [10] investigated MHD two-phase flow and heat transfer in an inclined channel. In another paper, Malashetty et al. [11] have studied the flow and heat transfer in an inclined channel containing fluid and porous layers. In recent years, the fluid flow and entropy generation in two immiscible fluids in an inclined/horizontal channel has received considerable attention by researchers. Komurgoz et al. [12] discussed second law analysis for an inclined channel containing porous-fluid layers by using the differential transform method. Kiwan and Khodier [13] discussed natural convection heat transfer in an open-ended inclined channel-partially filled with porous media.

Couple Stress Fluids: Since classical continuum mechanics of fluid does not consider size effect of particle additives in the fluid, it fails to define the features of such non-Newtonian fluids. Various theories have been postulated to interpret the rheological abnormalities which are due to the long chain molecules of the lubricant additives. The flow behavior of blended lubricants is well described by Stokes micro continuum theory [14, 15], which considers the polar effects, such as presence of non-symmetric stress tensors, couples tresses (i.e. stress produced due to spin of micro elements in the fluid) and body couples in the fluid. This theory is referred as couple stress theory of fluids among the research community. Mineral oils containing polar compounds (like polymer additive), synthetic lubricant, colloidal fluids, liquid crystals, and bio-fluids (blood [16], synovial fluid [17]) are the examples of couple stress fluid. The study of couple-stress fluids has applications in a number of processes that occur in various industries such as the extrusion of polymer fluids, solidification of liquid crystals, cooling of metallic plate in a bath, colloidal solutions etc. Stokes discussed the hydro-magnetic steady flow of a fluid with couple stress effects. A review of couple stress (polar) fluid dynamics was reported by Stokes [15]. Soundalgekar and Aranake [18] discussed the effects of couple stresses on MHD Couette flow. Application of the couple stress fluid model to biomechanics problems has been proposed in the study of peristaltic transport by Srivastava [19]. Shehawey and Mekheimer [20] and blood flow in the microcirculation by Dulal Pal et al. [21]. Many authors have investigated the couple stress effects with reference to different lubrication problems (Hsiu-Lu Chiang [22], Naduvinamani et al. [23], Jian and Chen [24], Lu and Lin [25]).

Homotopy Analysis Method: In recent years, a growing interest towards the application of the homotopy technique in nonlinear problems has been devoted by the engineering practice. The main success of the HAM consists in the fact that a simple problem is to continuously deform to solve into the difficult problem under study. The homotopy analysis method (HAM), first proposed by Liao [26, 27] is one of the most successful and efficient methods in solving different types of nonlinear differential equations such as coupled, decoupled, homogeneous and non-homogeneous. This method does not require small/large parameters and thus can be applied to solve nonlinear problems without small or large parameters. Its main procedure is to construct a class of homotopy in a very general form by introducing an auxiliary parameter. This parameter can provide us with a convenient way to control the convergence of approximation series and adjust convergence regions when necessary. The description of this method was given systematically by Liao [28], where the author also discussed the convergence of the approximation series and showed that, as long as the series given by HAM converges, it must converge to one solution of the studied problem.

Thermodynamic analysis in the case of viscous fluids was carried out by many researchers. But very less attention has been paid in this direction for the couple stress fluid flows. Since couple stress fluids are known to have rotational effects, these fluids may help to increase the exergy. Hence, in the present study, attention is paid to examine the entropy generation characteristics for an inclined channel of two immiscible couple stress fluids.

MATHEMATICAL FORMULATION AND GOVERNING EQUATIONS

Consider a steady, fully developed laminar flow of two immiscible couple stress fluids between two inclined parallel plates distant 2h apart. Choose the coordinate system such that X-axis is taken along horizontal direction through the central line of the channel, Y is perpendicular to the plates and the two plates are infinitely extended in the direction of X (Figure 1). The length of the plates is much greater than the distance between them so that the flow at any point in the X-direction is same. Since the boundaries in the X direction are of infinite dimensions, without loss of generality, we assume that the physical quantities depend on Y only. Fluid flow is generated due to a constant pressure gradient which acts at the mouth of the channel. The fluid in the lower zone (viscosity μ_1, density ρ_1 and thermal conductivity k_1) occupies the region ($-h \le Y \le 0$) comprising the lower half of the channel and this region will be referred to as zone I. The fluid in the upper zone (viscosity μ_2, density ρ_2 ($<\rho_1$) and thermal conductivity k_2) is assumed to occupy the upper half of the channel (i.e., $0 \le Y \le h$), and this region is called zone II. The two walls of the channel are held at different temperatures T_I and T_{II} (with $T_I < T_{II}$). Also, the tilt angle, measured clockwise from the horizontal is denoted by φ in the considered equations. The fluid properties are assumed to be constant except for density variations in the buoyancy force term. The equations for the flow in zone I and II (i.e., $-h \le Y \le h$) are assumed to be governed by couple stress fluid flow equations (neglecting body forces except gravity force and body couples) of Stokes [14, 15] and energy equation

$$\frac{d\rho}{dt}+\nabla.(\rho\bar{q})=0 \tag{1}$$

$$\rho\left[\frac{d\bar{q}}{dt}+(\bar{q}\cdot\nabla)\bar{q}\right]=\rho\bar{f}+\frac{1}{2}\nabla\times(\rho\bar{l})-\nabla P+\mu\nabla\times(\nabla\times\bar{q}) \\ -\eta\nabla\times(\nabla\times(\nabla\times(\nabla\times\bar{q})))+(\lambda+2\mu)\nabla(\nabla\cdot\bar{q})+\rho\bar{g} \tag{2}$$

$$\rho\frac{dE}{dt}=\Phi+k\nabla^2 T \tag{3}$$

$$\text{where } \Phi=\mu\left[(\nabla\bar{q}):(\nabla\bar{q})^T+(\nabla\bar{q}):(\nabla\bar{q})\right] \\ +4\eta\left[(\nabla\bar{\omega}):(\nabla\bar{\omega})^T\right]+4\eta'\left[(\nabla\bar{\omega}):(\nabla\bar{\omega})\right]$$

where $\bar{q}$ is the velocity vector, $\bar{\omega}=\frac{1}{2}(\nabla\times\bar{q})$ is the spin vector. The scalar quantity ρ is the density, P is the fluid pressure at any point. The material constants λ and μ are the viscosity coefficients and η and η' are the couple stress viscosity coefficients satisfying the constraints $\mu \ge 0$; $3\lambda+2\mu\ge 0$; $\eta\ge 0$, $|\eta'| \le \eta$. There is a length parameter $l=\sqrt{\eta/\mu}$ which is a characteristic measure of the polarity of the couple stress fluid and this parameter is identically zero in the case of non-polar fluids. In linear momentum equation (2), the body force term $\rho\bar{g}$ is taken as $\rho\bar{g}\,b(T-T_W)\sin\varphi$ for buoyancy force in case of heat conduction. In the energy equation, Φ is the dissipation function of mechanical energy per unit mass, E is the specific internal energy, $\bar{\mathbf{h}} = -k\ \nabla T$ is the heat flux, where k is the thermal conductivity and T is the temperature.

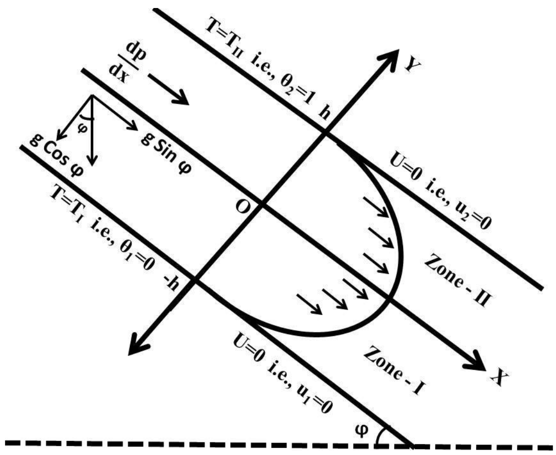

Figure 1 Schematic of the investigated problem

Herein the velocity vector $\bar{q}$ is taken in the form $\bar{q}$=(U(Y),0,0). Introducing the non-dimensional variables: $x = \frac{X}{h}, y = \frac{Y}{h}, u = \frac{U}{U_o}, p = \frac{P}{\rho_1 U_o^2}$ and $\theta = \frac{T - T_I}{T_{II} - T_I}$ where

U_o is the maximum velocity of the fluid in the channel.

The equations (2) and (3) reduced to the following sets of non-dimensional form of governing equations and boundary conditions corresponding to the flow in the two zones.

Zone I: (-1≤y≤0)

The governing equations in zone I are:

$$\frac{d^4 u_1}{dy^4} - s_1 \frac{d^2 u_1}{dy^2} - \frac{Gr}{Re} s_1 \theta_1 \operatorname{Sin}\varphi = -Re s_1 \frac{dp}{dx} \tag{4}$$

$$\frac{d^2 \theta_1}{dy^2} + Br\left[\left(\frac{du_1}{dy}\right)^2 + \frac{1}{s_1}\left(\frac{d^2 u_1}{dy^2}\right)^2\right] = 0 \tag{5}$$

Zone I: (0≤y≤1)

The governing equations in zone II are:

$$\frac{d^4 u_2}{dy^4} - s_2 \frac{d^2 u_2}{dy^2} - \frac{n_b n_\rho}{n_\mu} \frac{Gr}{Re} s_2 \theta_2 \operatorname{Sin}\varphi = -\frac{1}{n_\mu} Re\ s_2 \frac{dp}{dx} \tag{6}$$

$$\frac{d^2 \theta_2}{dy^2} + \frac{Br\, n_\mu}{n_k}\left[\left(\frac{du_2}{dy}\right)^2 + \frac{1}{s_2}\left(\frac{d^2 u_2}{dy^2}\right)^2\right] = 0 \tag{7}$$

Where $Re = \frac{\rho_1 U_o h}{\mu_1}$ is the Reynolds number, $s_i = \frac{\mu_i h^2}{\eta_i}$ is the couple stress parameter, Br = Ek Pr is the Brinkman number, $n_\mu = \frac{\mu_2}{\mu_1}$ is the viscosity ratio, $Ek = \frac{U_o^2}{c_{p1}(T_{II} - T_I)}$ is the Eckert number, $Gr = \frac{\rho_1^2 g b_1 h^3 (T_{II} - T_I)}{\mu_1^2} \operatorname{Sin}\varphi$ is the Grashof number, $Pr = \frac{\mu_1 c_{p1}}{k_1}$ is the Prandtl number, $n_b = \frac{b_2}{b_1}$ is the thermal expansion coefficient ratio, $n_\rho = \frac{\rho_2}{\rho_1}$ is the density ratio, $n_k = \frac{k_2}{k_1}$ is the thermal conductivity ratio (i=1,2).

BOUNDARY AND INTERFACE CONDITIONS:

A characteristic feature of the two-layer flow problem is the coupling across liquid/liquid interface. The liquid layers are mechanically coupled via transfer of momentum across the interface. Transfer of momentum results from the continuity of interface tangential velocity and from a stress balance across the interface. The above equations (4)-(7) are solved using appropriate boundary conditions.

To determine the velocity components $u_1(y)$, $u_2(y)$ in the zones I and II described above, we adopt the following boundary and interface conditions:

Zone I is constituted by the fixed lower plate given by y = −1 and a fluid-fluid interface defined by y = 0. Zone II is constituted by the fluid interface given by y = 0 and the fixed upper plate given by y = 1.

In view of the no slip condition on the static boundaries, we have to prescribe

$u_1(y) = 0$ on $y = -1$ and $u_2(y) = 0$ on $y = 1$ (8)

which represent the no slip condition.

Stokes mainly proposed two types of boundary conditions (A) and (B) respectively and the vanishing of couple stresses on the boundary is condition (A) [15]. This condition is adopted here as this is appropriate in the present context. On the static boundary, this leads to

$$\frac{d^2 u_1}{dy^2} = 0 \text{ on } y=-1 \text{ and } \frac{d^2 u_2}{dy^2} = 0 \text{ on } y=1 \tag{9}$$

At the fluid-fluid interface y = 0, we assume that the velocity, vorticity, shear stress and couple stress components are continuous. This implies

$$u_{1(0^-)} = u_{2(0^+)}, \left.\frac{du_1}{dy}\right|_{(0^-)} = \left.\frac{du_2}{dy}\right|_{(0^+)},$$

$$\left.\tau_{1xy}\right|_{(0^-)} = \left.\tau_{2xy}\right|_{(0^+)} \text{ and } M_{1xy(0^-)} = M_{2xy(0^+)} \tag{10}$$

The last two conditions of (10) give us $\left(s_1\frac{du_1}{dy}-\frac{d^3u_1}{dy^3}\right)_{(0^-)}=n_\eta\left(s_2\frac{du_2}{dy}-\frac{d^3u_2}{dy^3}\right)_{(0^+)}$ and

$\left(\frac{d^2u_1}{dy^2}\right)_{(0^-)}=n_\eta\left(\frac{d^2u_2}{dy^2}\right)_{(0^+)}$ respectively, where $n_\eta=\frac{\eta_2}{\eta_1}$ is the couple stress coefficient ratio.

The boundary conditions for temperature and heat flux at the plates and interface are as follows:
(i) at the lower and upper plate boundaries the temperatures are respectively,

$$\theta_1(y)=0 \text{ and } y=-1 \text{ and } \theta_2(y)=1 \text{ at } y=1 \tag{11}$$

(ii) at the fluid interface temperature (θ) and heat flux ($\bar{h}$) are continuous:

$$\theta_1(y)=\theta_2(y) \text{ and } \frac{d\theta_1}{dy}=n_k\frac{d\theta_2}{dy} \text{ at } y=0 \tag{12}$$

The equations for u and θ in (4) - (7) under the conditions (8) - (12) are solved by Homotopy Analysis Method (HAM).

HAM SOLUTION FOR VELOCITY AND TEMPERATURE PROFILES

zero-th order deformation equations

The homotopy equations for velocity u and temperature θ for both the zones is given by

$$(1\text{-}q)L_1\left[u_i(y;q)\text{-}u_o(y)\right]=q\,h_u\,N_1\left[u(y;q)\right],i=1,2 \tag{13}$$

$$(1\text{-}q)L_2\left[\theta_i(y;q)\text{-}\theta_o(y)\right]=q\,h_\theta\,N_2\left[\theta(y;q)\right],i=1,2 \tag{14}$$

where $q\in[0,1]$ is the embedding homotopy parameter.
The auxiliary operator is chosen as

$$L_1=\frac{\partial^4}{\partial y^4} \text{ and } L_2=\frac{\partial^2}{\partial y^2} \tag{15}$$

Such that

$$L\left(d_1+d_2y+d_3\frac{y^2}{2}+d_4\frac{y^3}{6}\right)=0 \text{ and } L(d_1+d_2y)=0 \tag{16}$$

and non-linear operators N_1 and N_2 are defined as

ZoneI:

$$N_1\left[u(y;q),\theta(y;q)\right]=\frac{d^4u_1}{dy^4}-s_1\frac{d^2u_1}{dy^2}-\frac{Gr}{Re}s_1\theta_1(y;q)\mathrm{Sin}\,\varphi+\mathrm{Res}_1\frac{dp}{dx} \tag{17}$$

$$N_2\left[u(y;q),\theta(y;q)\right]=\frac{d^2\theta_1(y;q)}{dy^2}+Br\left[\left(\frac{du_1(y;q)}{dy}\right)^2+\frac{1}{s_1}\left(\frac{d^2u_1(y;q)}{dy^2}\right)^2\right] \tag{18}$$

Zone II:

$$N_1\left[u(y;q),\theta(y;q)\right]=\frac{d^4u_2}{dy^4}-s_2\frac{d^2u_2}{dy^2}-\frac{n_b\,n_\rho}{n_\mu}\frac{Gr}{Re}s_2\theta_2(y;q)\mathrm{Sin}\,\varphi+\frac{1}{n_\mu}\mathrm{Res}_2\frac{dp}{dx} \tag{19}$$

$$N_2\left[u(y;q),\theta(y;q)\right]=\frac{d^2\theta_2(y;q)}{dy^2}+\frac{Br\,n\mu}{n_k}\left[\left(\frac{du_2(y;q)}{dy}\right)^2+\frac{1}{s_2}\left(\frac{d^2u_2(y;q)}{dy^2}\right)^2\right] \tag{20}$$

For HAM solutions, we choose the initial approximations of u(y) and θ(y) in both the zones as follows

$$u_1(y;0)=u_{1,0}(y)=0,\theta_1(y;0)=\theta_{1,0}(y)=\frac{n_k(y+1)}{1+n_k},$$

$$u_2(y;0)=u_{2,0}(y)=0,\theta_2(y;0)=\theta_{2,0}(y)=\frac{(y+n_k)}{1+n_k} \tag{21}$$

and satisfying the boundary conditions

$$u_{1,0}(-1)=0,u_{1,0}(1)=0,\frac{d^2u_{1,0}(-1)}{dy^2}=0,\frac{d^2u_{2,0}(1)}{dy^2}=0,u_{1,0}(0)=u_{2,0}(0),$$

$$\frac{du_{1,0}(0)}{dy}=\frac{du_{2,0}(0)}{dy},\frac{d^2u_{1,0}(0)}{dy^2}=n_\eta\frac{d^2u_{2,0}(0)}{dy^2},\tau_{xy}|_{1,0}=\tau_{xy}|_{2,0}, \tag{22}$$

$$\theta_{1,0}(-1)=0,\ \theta_{1,0}(1)=0,\ \theta_{1,0}(0)=\theta_{2,0}(0) \text{ and } \frac{d\theta_{1,0}(0)}{dy}=n_k\frac{d\theta_{2,0}(0)}{dy}$$

When q = 1, Eqns. (13) - (14) are same as Eqns. (4) - (7) respectively, therefore at q = 1 we get the final solutions

$$u_1(y,1)=u_1(y),\theta_1(y,1)=\theta_1(y),u_2(y,1)=u_2(y),\theta_2(y,1)=\theta_2(y) \tag{23}$$

Hence the process of giving an increment to q from 0 to 1 is the process of $u_1(y;q)$ varying continuously from the initial guess $u_{1,0}(y)$ to the final solution $u_1(y)$ (similar for $\theta_1(y)$, $u_2(y)$ and $\theta_2(y)$). This kind of continuous variation is called deformation in topology so that we call system Eqns. (13) - (14), the zero-th order deformation equations.

m-th order deformation equations

The m-th order deformation equations can be written as

$$L_1\left[u_{i,m}-\chi_m u_{i,m-1}(y)\right]=h_uR^u_{i,m}(y) \tag{24}$$

$$L_2\left[\theta_{i,m}-\chi_m\theta_{i,m-1}(y)\right]=h_\theta R^\theta_{i,m}(y) \tag{25}$$

with the boundary conditions of

$$u_{1,m}(-1)=0,u_{1,m}(1)=0,\frac{d^2u_{1,m}(-1)}{dy^2}=0,\ \frac{d^2u_{2,m}(1)}{dy^2}=0,u_{1,m}(0)=u_{2,m}(0),$$

$$\frac{du_{1,m}(0)}{dy}=\frac{du_{2,m}(0)}{dy},\frac{d^2u_{1,m}(0)}{dy^2}=n_\eta\frac{d^2u_{2,m}(0)}{dy^2},\tau_{xy}\big|_{1,m}=\tau_{xy}\big|_{2,m},$$

$$\theta_{1,m}(-1)=0,\theta_{1,m}(1)=0,\theta_{1,m}(0)=\theta_{2,m}(0),\frac{d\theta_{1,m}}{dy}=n_k\frac{d\theta_{2,m}}{dy} \tag{26}$$

Where

$$R^u_{1,m}(y)=\frac{d^4u_{1,m-1}(y;q)}{dy^4}-s_1\frac{d^2u_{1,m-1}(y;q)}{dy^2}-\frac{Gr}{Re}s_1\theta_{1,m-1}(y;q)\mathrm{Sin}\,\varphi+\mathrm{Re}\,s_1\frac{dp}{dx} \tag{27}$$

$$R_{1,m}^{\theta}(y) = \frac{d^2\theta_{1,m-1}(y;q)}{dy^2} + Br\left[\sum_{n=0}^{m-1}\left(\frac{du_{1,n}(y;q)}{dy}\frac{du_{1,(m-1)-n}(y;q)}{dy}\right) + \frac{1}{s_1}\sum_{n=0}^{m-1}\left(\frac{d^2u_{1,n}(y;q)}{dy^2}\frac{d^2u_{1,(m-1)-n}(y;q)}{dy^2}\right)\right] \tag{28}$$

$$R_{2,m}^{u}(y) = \frac{d^4u_{2,m-1}(y;q)}{dy^4} - s_2\frac{d^2u_{2,m-1}(y;q)}{dy^2} - \frac{n_b n_\rho}{n_\mu}\frac{Gr}{Re}s_2\,\theta_{2,m-1}(y;q)\sin\phi + \frac{1}{n_\mu}Re\,s_2\frac{dp}{dx} \tag{29}$$

$$R_{2,m}^{\theta}(y) = \frac{d^2\theta_{2,m-1}(y;q)}{dy^2} + \frac{Br\,n_\mu}{n_k}\left[\sum_{n=0}^{m-1}\left(\frac{du_{2,n}(y;q)}{dy}\frac{du_{2,(m-1)-n}(y;q)}{dy}\right) + \frac{1}{s_2}\sum_{n=0}^{m-1}\left(\frac{d^2u_{2,n}(y;q)}{dy^2}\frac{d^2u_{2,(m-1)-n}(y;q)}{dy^2}\right)\right] \tag{30}$$

For m being integer $\chi_m = 0$, for $m \le 1$ and $\chi_m = 1$, for $m > 1$

The initial guess approximations $u_{1,0}(y)$, $\theta_{1,0}(y)$, $u_{2,0}(y)$, and $\theta_{2,0}(y)$, linear operators L_1 and L_2 and the auxiliary parameters h_u and h_θ are assumed to be so selected that Eqns. (13) - (14) have solution at each point $q \in [0, 1]$. With the help of Taylors series and by referring to Eqn. (22), u(y; q), θ(y; q) can be expressed as

$$u_i(y;q) = \sum_{m=0}^{\infty} u_{i,m}(y)q^m, i = 1,2 \tag{31}$$

$$\theta_i(y;q) = \sum_{m=0}^{\infty} \theta_{i,m}(y)q^m, i = 1,2 \tag{32}$$

in which the convergence of series equations (31) - (32) depends strongly upon the auxiliary parameters h_u and h_θ-the values of h_u and h_θ are selected in such a way that the series equations (31) - (32) converge when q=1. Hence equations (31) - (32) become,

$$u_i(y) = \sum_{m=0}^{\infty} u_{1,m}(y), i = 1,2 \tag{33}$$

$$\theta_i(y) = \sum_{m=0}^{\infty} \theta_{i,m}(y), i = 1,2 \tag{34}$$

for which we presume that the initial guesses to u, θ satisfies L(u) = 0 and L(θ) = 0 and the non-zero auxiliary parameters h_u and h_θ are so selected.

The m-th order derivatives for u(y; q), θ(y; q) are defined as

$$u_{i,m}(y) = \frac{1}{m!}\frac{\partial^m u_i(y;q)}{\partial q^m}, \theta_{i,m}(y) = \frac{1}{m!}\frac{\partial^m \theta_i(y;q)}{\partial q^m}, i = 1,2$$

It is clear that the convergence of Taylor series at q = 1 is a prior assumption, whose justification is provided via a theorem [30]. The effects of relevant parameters in flow two immiscible couple stress fluids can be studied from the exact formulas (31) - (32). Moreover, a special emphasize should be placed here that the m-th order deformation system (24) - (25) is a linear differential equation system with an auxiliary linear operators L whose fundamental solution is known.

ENTROPY GENERATION ANALYSIS

The volumetric entropy generation

It is assumed that each the couple stress fluid with the constant physical properties (ρ_i, μ_i, η_i, k_i, cp_i) is flowing in the channel subjected to constant wall temperatures on the each plate. If we take an infinitesimal fluid element in each zone and assume that the element as an open thermodynamic system subjected to mass fluxes, energy transfer and entropy transfer interactions through a fixed control surface, the volumetric rate of entropy generation for incompressible couple stress fluid is given as

$$(S_i)_G = (Si)_{G,\,heat\ transfer} + (Si)_{G,\,viscous\ dissipation} = \frac{k}{T_o^2}\left(\frac{\partial T}{\partial y}\right)^2 + \frac{1}{T_o}\Phi$$

Where Φ is the viscous dissipation function.
For the present study, the volumetric rate of entropy generation reduces to

$$(S_i)_G = \frac{k_i}{T_o^2}\left(\frac{\partial T_i}{\partial Y}\right)^2 + \frac{\mu_i}{T_o}\left(\frac{\partial U_i}{\partial Y}\right)^2 + \frac{\eta_i}{T_o}\left(\frac{\partial^2 U_i}{\partial Y^2}\right)^2 \tag{35}$$

where the value of i can be either 1 or 2 that represents fluid I or fluid II, respectively. On the right hand side of the above equation, the first term is the entropy generation due to heat conduction and the remaining two terms represent entropy generation due to the viscous dissipation function Φ for an incompressible couple stress fluid. Entropy generation rate is positive and finite as long as temperature and velocity gradients are present in the medium.

The characteristic entropy generation rate

The characteristic entropy generation rate $S_{G,C}$ is defined as,

$$S_{G,C} = \left[\frac{(\bar{h}_1)^2}{k_1 T_o^2}\right] = \left[\frac{k_1(\Delta T)^2}{h^2 T_o^2}\right] \tag{36}$$

In the above equation, $\bar{h}_1$ is the heat flux in zone I, T_o is the average, characteristic, absolute reference temperature of the medium, $\Delta T = T_{II} - T_I$ and h is the half of transverse distance of the channel.

The entropy generation number

The entropy generation number for each fluid with dimensionless variables are given by

$$Ns_1 = \frac{(S_1)_G}{S_{G,C}} = \left(\frac{d\theta_1}{dy}\right)^2 + \left(\frac{Br}{\Omega}\right)\left[\left(\frac{du_1}{dy}\right)^2 + \frac{1}{s_1}\left(\frac{d^2u_1}{dy^2}\right)^2\right] \tag{37}$$

$$Ns_2 = \frac{(S_2)_G}{S_{G,C}} = \left(\frac{d\theta_2}{dy}\right)^2 + \left(\frac{Br}{\Omega}\right)\frac{n_\mu}{n_k}\left[\left(\frac{du_2}{dy}\right)^2 + \frac{1}{s_2}\left(\frac{d^2u_2}{dy^2}\right)^2\right] \tag{38}$$

where $Br = \left(\frac{\mu_1 U_o^2}{k_1 \Delta T}\right)$ is the Brinkman number, which determines the importance of viscous dissipation because of the fluid frictions relative to the conduction heat flow resulting from the impressed temperature difference and $\Omega = \left(\Delta T / T_o\right)$ is the dimensionless temperature difference.

Fluid friction versus heat transfer irreversibility

Entropy generation number (Ns) is good for generating entropy generation profiles but fails to give any idea about relative importance of friction and heat transfer effects. Two alternate parameters, irreversibility distribution ratio (ϕ) and Bejan number (Be), are introduced for this purpose and they are achieving an increasing popularity among researchers studying the second law.

The irreversibility ratio

The idea of irreversibility distribution ratio ϕ can enhance the understanding of the irreversibilities associated with the heat transfer and the fluid friction. It is defined as the ratio of entropy generation due to fluid frictions (Nf) to heat transfer in transverse direction (Ny) i.e,

$$\phi = \frac{S_{G,\text{fluid friction}}}{S_{G,\text{heat transfer}}} = \left(\frac{Nf}{Ny}\right)$$

ϕ can be interpreted as follows: If $0 \le \phi < 1$, then ϕ indicates that heat transfer irreversibility dominates and if $\phi > 1$ the fluid friction dominates. For the case of $\phi = 1$, both the heat transfer and fluid friction have the same contribution for entropy generation.

The Bejan number

An alternative irreversibility distribution parameter, called Bejan number Be, was defined by Paoletti et al., [29] as ratio of entropy generation due to heat transfer to the total entropy generation and it is given by

$$Be = \frac{\text{entropy generation due to heat transfer}}{\text{total entropy generation}} = \frac{Ny}{Ns} = \frac{Ny}{Ny + Nf} = \frac{1}{1+\phi}$$

The value of Be $\rightarrow$ 1 indicates that the heat transfer irreversibility dominates over fluid friction, and this corresponds to the case of $\phi \rightarrow 0$. On the other hand, Be $\rightarrow$ 0 indicates that the irreversibility due to fluid friction and magnetic field dominates over the irreversibility due to the heat transfer. This corresponds to $\phi \rightarrow 1$. It is obvious that Be = 0.5 is the case at which the heat transfer and fluid friction entropy generation rates are equal, and this corresponds to the case of ϕ= 1.

Importance of second law: By the first law of thermodynamics, we can find the temperature distributions of fluids within the channel and also heat transfer coefficients at the walls. But this law will not give any information regarding the relative effects of viscosity and heat convection for entropy generation. Second law states that entropy is always positive. The law is also stated in the form of inequality in terms of entropy generation. It can be noted that the second law analysis makes it possible to compare many different interactions in a system, and to identify the major sources of exergy destructions/losses. This enables us to identify the region where exactly the entropy generation is more in the entire fluid regime.

CONVERGENCE OF THE HAM SOLUTION

h-curves:

HAM provides us with a great freedom in choosing the solution of a nonlinear problem by different base functions. This has a great effect on the convergence region because the convergence region and the rate of a series are chiefly determined by the base functions used to express the solution. Therefore, we can approximate a nonlinear problem more efficiently by choosing a proper set of base functions and ensure its convergency. On the other hand, as pointed out by Liao [31], the convergence and rate of approximation for the HAM solution strongly depends on the value of auxiliary parameter h. By means of the so-called h-curves, it is easy to find out the so-called valid regions of auxiliary parameters to gain a convergent series solution. The expressions for u and θ contain the auxiliary parameters h_u and h_θ. The h-curves are plotted by choosing h_u and h_θ in such a manner that the solutions (33) - (34) ensure convergence [27]. Here to see the admissible values of h_u and h_θ, the h-curves are plotted for 15th order of approximation in Figures 2 - 3 by taking the values of the parameters as: B = 0.1, Br = 0.1, Gr = 0.2, n_β = 0.8, n_k = 0.8, n_μ = 0.8, n_η = 0.8, φ= $\pi/4$, Re = 2, s_1 = 1.2, and s_2 = 1.2. Clearly from the Figs. 2a and 2b, it is found that the admissible ranges of h_u and h_θ are $-1.6 < h_u < 0$ and $-1.8 < h_\theta < 0.3$ respectively. A wide valid zone is evident in these figures ensuring convergence of the series.

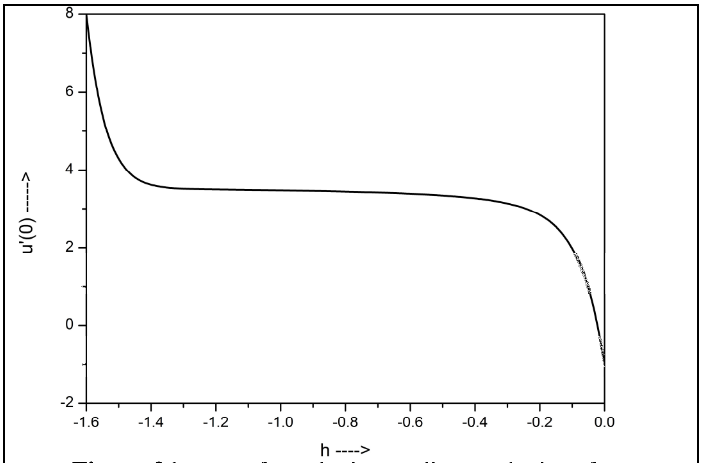

Figure 2 h-curve for velocity gradient at the interface

RESULTS AND DISCUSSION

The solutions for u_1, θ_1, u_2, θ_2 have been computed and shown graphically in Figures. The effects of couples stress parameter s_2, Reynolds number Re, Grashof number Gr, viscous dissipation parameter (Br/Ω) on velocity u, temperature θ, entropy generation number Ns and Bejan number Be have been studied.

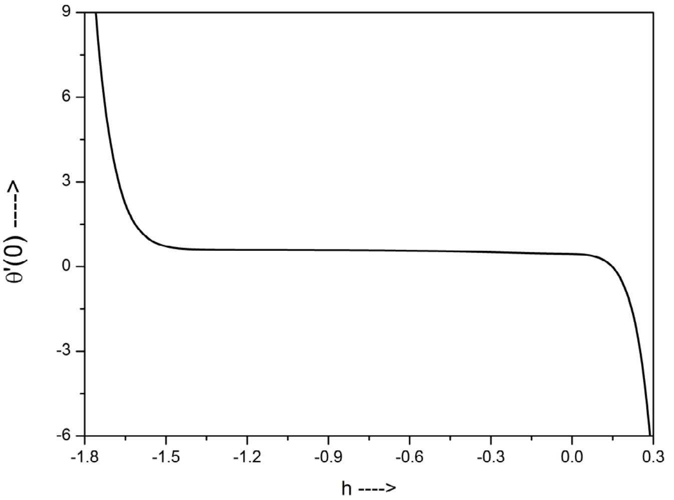

Figure 3 h-curve for temperature gradient at the interface

Effect of couple stress parameter (s_2):

From Figures 4, 5 and 7 we notice that as couple stress parameter s_2 increases, velocity, temperature and Bejan number are increasing. As $s_2 \to \infty$ we get the case of viscous fluid. In couple stress fluids a part of energy is used for rotation of the particles and creates couple stresses. Since in viscous fluids, rotation of particles is not considered. Hence, the velocity of viscous fluid is more than that of couple stress fluid (see Fig.4). The temperature due to dissipation of energy (depending on velocity) changes very slightly (see Figure 5). The same effect is seen on the entropy generation number Ns in Figure 6. But near the plates effect of couple stresses on Ns is considerable. This may be due to more friction near the walls. From Figure 7, we see that Bejan number is high at the interface. From the limiting case of $s_2 \to \infty$, we see that Be for viscous fluids is less than that of couple stress fluids. A slight increase in couple stress parameter s_2, increases Bejan number Be very much at the interface. Since Be is minimum near to the plates, entropy generation rate in transverse direction is also maximum (at the plate) and hence fluid friction dominates near to the plates.

Effect of Reynolds number (Re):

Figure 8 shows that as Re increases, Ns increases. Also it is observed that from the equations (37) and (38), the larger is the velocity and temperature gradients, the larger is the entropy generation rate. Figure 9 illustrates that as Re increases, Be decreases. This implies that in the entire flow region, as Re increases the relative increase of dissipation of energy due to friction dominates the dissipation of energy due to heat transverse flow. The variation of Be near the plates is more than what it is at the interface. This indicates that frictional forces are increasing rapidly near the walls.

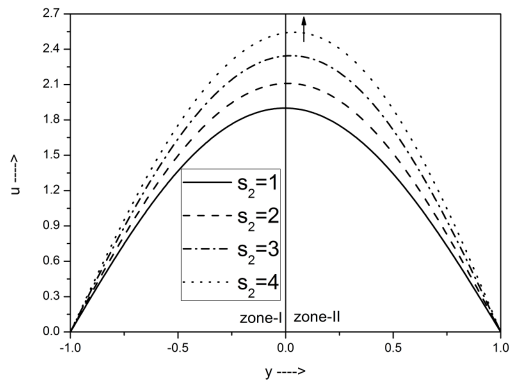

Figure 4 Effect couple stress parameter s_2 on velocity u for B=-0.3, Br=0.1, Gr=1.5, n_β=0.9, n_η=0.9, n_k=0.9, n_μ=0.9, $\varphi = \pi/4$, Re=1, s_1=2.

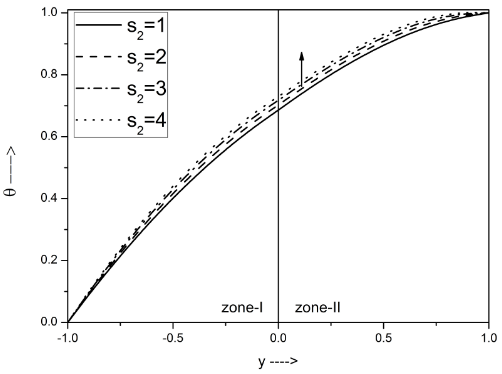

Figure 5 Effect couple stress parameter s_2 on temperature θ for B=-0.3, Br=0.1, Gr=1.5, n_β=0.9, n_η=0.9, n_k=0.9, n_μ=0.9, $\varphi = \pi/4$, Re=1, s_1=2.

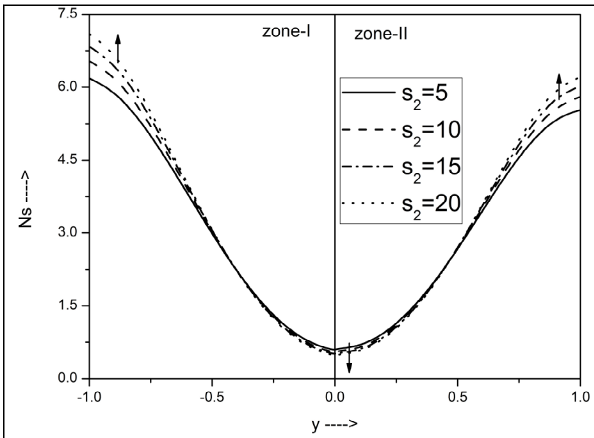

Figure 6 Effect couple stress parameter s_2 on entropy generation number Ns for B=-0.6, Br=0.1, Gr=0.1, n_β=0.9, n_η=0.9, n_k=1, n_μ=0.9, $\varphi = \pi/4$, Re=1, s_1=5, Ω=1.

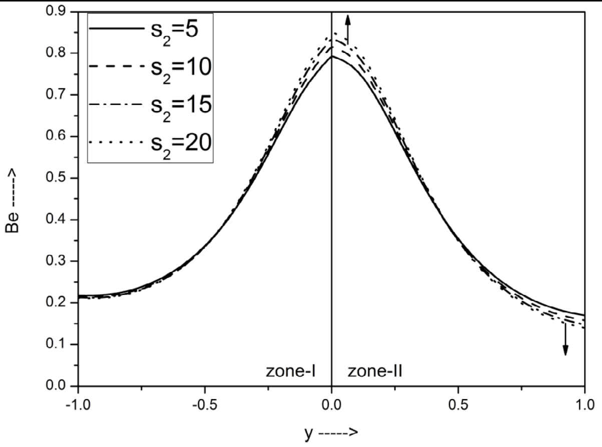

Figure 7 Effect couple stress parameter s_2 on Bejan number Be for B=-0.6, Br=0.1, Gr=0.1, n_β=0.9, n_η=0.9, n_k=1, n_μ=0.9, $\varphi=\pi/4$, Re=1, s_1=5, Ω=1.

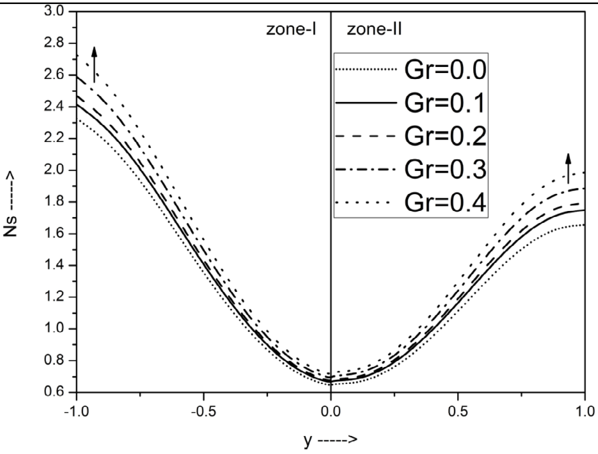

Figure 10 Effect Grashof number Gr on entropy generation number Ns for B=-0.8, Br=0.1, n_β=0.9, n_η=0.9, n_k=1.5, n_μ=0.9, $\varphi=\pi/4$, Re=0.5, s_1=8, s_2=8, Ω=1.

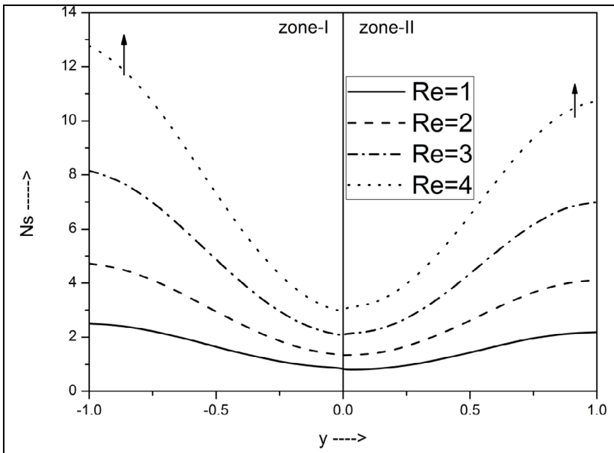

Figure 8 Effect Reynolds number Re on entropy generation number Ns for B=-0.5, Br=0.1, Gr=0.1, n_β=0.9, n_η=0.9, n_k=1.5, n_μ=0.9, $\varphi=\pi/4$, s_1=8, s_2=8, Ω=1.

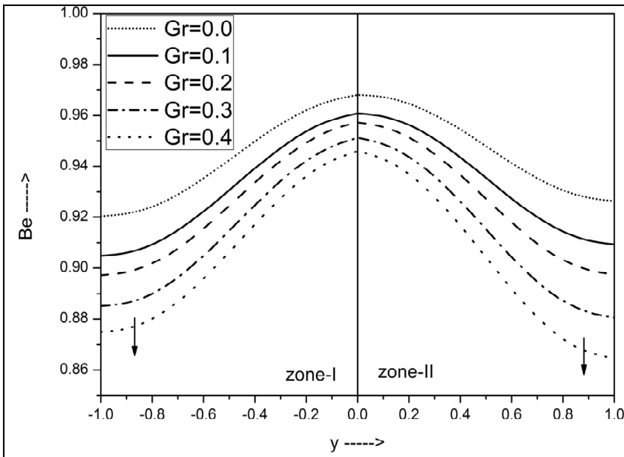

Figure 11 Effect Grashof number Gr on Bejan number Be for B=-0.8, Br=0.1, n_β=0.9, n_η=0.9, n_k=1.5, n_μ=0.9, $\varphi=\pi/4$, Re=0.5, s_1=8, s_2=8, Ω=1.

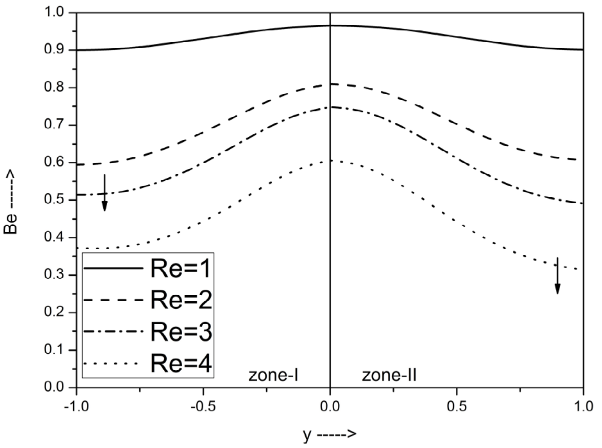

Figure 9 Effect Reynolds number Re on Bejan number Be for B=-0.5, Br=0.1, Gr=0.1, n_β=0.9, n_η=0.9, n_k=1.5, n_μ=0.9, $\varphi=\pi/4$, s_1=8, s_2=8, Ω=1.

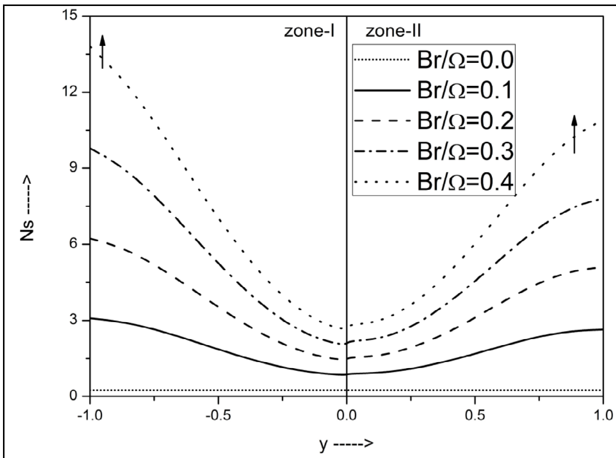

Figure 12 Effect viscous dissipation parameter (Br/Ω) on entropy generation number Ns for B=-0.5, Gr=0.1, n_β=0.9, n_η=0.9, n_k=1, n_μ=0.9, $\varphi=\pi/4$, Re=1, s_1=8, s_2=8.

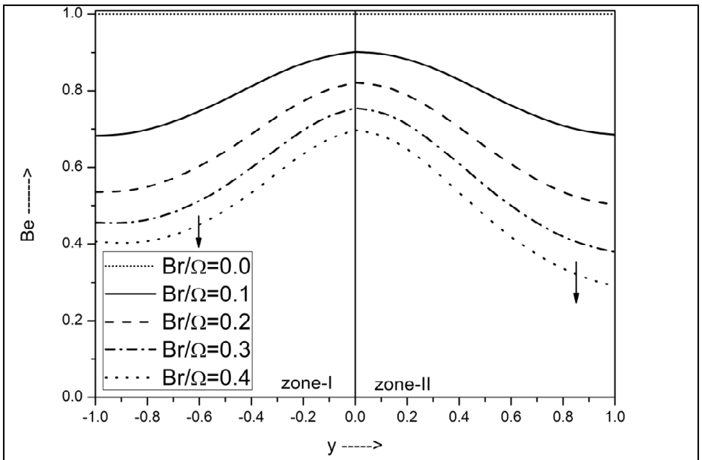

Figure 13 Effect viscous dissipation parameter (Br/Ω) on Bejan number Ns for B=-0.5, Gr=0.1, n_β=0.9, n_η=0.9, n_k=1, n_μ=0.9, φ= π/4, Re=1, s_1=8, s_2=8.

Effect of Grashof number (Gr):

From Figure 10, we notice that as Grashof number Gr increases, entropy generation number increases. But near the plates effect of Grashof number on Ns is considerable. This may be due to more friction near the walls. From Figure 11, we see that as Grashof number Gr increases, Bejan number Be decreases and keeping its value maximum at the interface. Be is more than 0.8 in the entire region of the channel. Effect of Grashof number due to fluid friction is small. At the interface Be attains value more than 0.9. Though as Gr increases, Be decreases, this decrease is not high. This may be due to the fact that flow generates naturally by gravitational pull.

Effect of viscous dissipation parameter (Br/Ω):

From Figure 12, we observe that as the viscous dissipation parameter (Br/Ω) increases, the entropy generation number Ns increases. The greater the viscosity of the fluid, the greater the entropy generation rate. It is observed that Ns≅0 at the interface of the channel. This implies that at the interface, entropy generation is minimum i.e., exergy is maximum (available energy) and hence the dissipation of energy is almost zero and the thermal process is almost reversible there. When (Br/Ω) → 0, the entropy generation number Ns → 1 and becomes independent of the transverse distance. This is an ideal case which corresponds to the energy due to only the heat conduction and the effect of viscous dissipation disappears. There is a lowest point of the entropy generation rate at each specified value of the viscous dissipation parameter and it occurs near the interface. The profiles indicate that at the interface y=0, the entropy generation rate is minimum and hence the available energy in the transverse direction is maximum.

From Figure 13, we observe that as the viscous dissipation parameter (Br/Ω) increases, Bejan number Be decreases. This shows that the Bejan number is maximum at the interface of the channel and decreases as we move towards the channel walls in either direction. We again observe that for (Br/Ω) = 0, Be is equal to its maximum theoretical value (Be=1), i.e., the fluid friction effect provides no contribution to the entropy generation. For all other values of (Br/Ω), the Bejan number has a maximum value close to the central line of the channel and then decreases near the walls.

CONCLUSIONS

In this study, the flow of immiscible couple stress fluids between two parallel plates due to the constant pressure gradient is studied. The approximate analytical series solutions are obtained applying homotopy analysis method (HAM). The exergy loss distribution is studied in terms of second law of thermodynamics. The entropy generation number Ns at every point y between the channels is found. The effect of viscous dissipation parameter (Br/Ω) on entropy generation number (Ns), Bejan number (Be) is studied through figures. From the present study we observe that:

1. The presence of couple stresses in the fluid decreases the velocity and temperature. (As s_2 increases, couple stresses decrease).
2. The entropy generation rate is more near the plates in zone I than that of zone II. This may be due to the fact that the fluid in the lower zone is more viscous. This indicates the more the viscosity of the fluid is, the more the entropy generation.
3. The entropy generation rate is minimum at the interface. This indicates that the fluid friction is minimum and exergy is maximum at the interface.
4. Grashof number Gr has little effect on the entropy generation rate.

ACKNOWLEDGEMENTS

The authors would like to thank the DST, Govt. of India for providing travel support from ITS scheme to present this paper in the conference.

REFERENCES

[1] Bejan A., A study of entropy generation in fundamental convective heat transfer, *Journal of Heat Transfer*, Vol. 101, 1979, pp. 718-725.

[2] Bejan A., Second law analysis in heat transfer, Energy, Vol. 5, 1980, pp. 721-732.

[3] Bejan A., Convection heat transfer, John Wiley and Sons, 2004.

[4] Baytas A.C., Entropy generation for natural convection in an inclined porous cavity, *International Journal of Heat and Mass Transfer*, Vol. 43, 2000, pp. 2089–2099.

[5] Saouli S., and Aiboud-Saouli S., Second law analysis of laminar falling liquid film along an inclined heated plate, *International Communications Heat Mass Transfer*, Vol. 31, 2004, pp. 879-886.

[6] Makinde O.D., Irreversibility analysis for gravity driven non-Newtonian liquid film along an inclined isothermal plate, *Physica Scripta*, vol. 74, 2006, pp. 642-645.

[7] Havzali M., Arikoglu A., Komurgoz G., Keser H.I., and Ozkol I., Analytical numerical analysis of entropy generation for gravity-driven inclined channel flow with initial transition and entrance effects, *Physica Scripta*. Vol. 78, 2008, Paper number 045401.

[8] Ibáñez, G., López, A., Pantoja, J. and Moreira, J., Combined effects of uniform heat flux boundary conditions and

hydrodynamic slip on entropy generation in a micro-channel, *International Journal of Heat and Mass Transfer,* Vol. 73, 2014, pp. 201-206.
[9] Bakhtiyarov S.I., and Siginer D.A., A note on the laminar core-annular flow of two immiscible fluids in a horizontal tube, *Proceed. Int. Symposium on liquid-liquid two phase flow and transport phenomena*, Begell house, Inc. Santa Barbara, 1997, pp. 107–111.
[10] Malashetty M.S., and Umavathi J.C., Two phase magneto-hydrodynamic flow and heat transfer in an inclined channel, *Internatinal Journal of Multiphase Flow*, Vol. 23(3) , 1997, pp. 545-560.
[11] Malashetty M.S., and Umavathi J.C., and Prathap Kumar J., Two fluid flow and heat transfer in an inclined channel containing porous and fluid layer, *Heat Mass Transfer*, Vol. 40, 2004, pp. 871-876.
[12] Komurgoz G., Arikoglu A., Turker, E., and Ozkol, I., Second law analysis for an inclined channel containing porous-clear fluid layers by using the differential transform method, *Numerical Heat Transfer, Part A: Applications: An International Journal of Computation and Methodology*, Vol. 57(8) , 2010, pp. 603-623.
[13] Kiwan, S., and Khodier, M., Natural convection heat transfer in an open-ended inclined channel-partially filled with porous media, *Heat Transfer Engineering*, Vol. 29(1), 2011, pp. 67-75.
[14] Stokes V.K., Couple stresses in fluid. *The Physics of Fluids*. Vol. 9(9), 1966, pp. 1709-1715.
[15] Stokes V.K., Theories of fluids with microstructures. Springer, NewYork, 1984.
[16] Srivastava L.M., Flow of couple stress fluid through stenotic blood vessels, *Journal of Biomechanics*, Vol. 18, 1985, Paper number 47985.
[17] Bujurke N.M., and Kudenatti R.B., An analysis of rough poro elastic bearings with reference to lubrication mechanism of synovial joints, *Applied Mathematics and Computation*, Vol. 178, 2006, pp. 30920.
[18] Soundalgekar V.M., and Aranake R.N., Effects of couple stresses on MHD Couette flow, *Nuclear Engineering and Design*, vol. 49, 1978, pp. 197–203.
[19] Srivastava L. M., Peristaltic transport of a couple stress fluid, *Rheologica Acta*, Vol. 25, 1986, pp. 638–641.
[20] Shehawey E.F.E., and Mekheimer K.S., Couple stresses in peristaltic transport of fluids, *Journal of Physics D: Applied Physics,* vol. 27, 1994, pp. 1163–1170.
[21] Dulal Pal., Rudraiah L.M., and Devanathan R., A couple stress model of blood flow in the microcirculation, *Bulletin of Mathematical Biology,* Vol. 50, 1988, pp. 329–344.
[22] Hsiu-Lu Chiang., Cheng-Hsing Hsu., and Jaw-Ren Lin., Lubrication performance of finite journal bearings considering effects of couple stresses and surface roughness, *Tribology International Journal*, Vol. 37(4), 2004, pp. 297-307.
[23] Naduvinamani N.B., Hanumagowda B.N., and Syeda Tasneem Fathima., Combined effects of MHD and surface roughness on couplestress squeeze film lubrication between porous circular stepped plates, *Tribology International,* Vol. 56, 2012, pp. 19–29.
[24] Cai-Wan Chang-Jian., and Chao-Kuang Chen., Chaos and bifurcation of a flexible rotor supported by porous squeeze couple stress fluid film journal bearings with non-linear suspension, *Chaos, Solitons & Fractals*, Vol. 35(2), 2006, pp. 358–375.
[25] Lu R. F., and Lin J. R., A theoretical study of combined effects of non-Newtonian rheology and viscosity pressure dependence in the Sphere-plate squeeze-film system, *Tribology International Journal,* Vol. 40, 2007, pp. 125–131.
[26] Liao S.J., The proposed homotopy analysis technique for the solution of nonlinear problems, *PhD Thesis*, Shanghai Jiao Tong University, 1992.
[27] Liao S.J., Beyond perturbation: Introduction to homotopy analysis method, Boca Raton: Chapman and Hall-CRC Press, 2003.
[28] Liao S.J., An explicit, totally analytic approximate solution for Blasius viscous flow problems, *International Journal of Non-linear Mech*anics, Vol. 34, 1999, pp. 759-778.
[29] Paoletti S., Rispoli F., and Sciubba E., Calculation exergetic loses in compact heat exchanger passages, *ASME AES*, Vol. 10(2), 1989, pp. 21–29.
[30] Turkyilmazoglu, M. Numerical and analytical solutions for the flow and heat transfer near the equator of an MHD boundary layer over a porous rotating sphere. *International Journal of Thermal* Sciences, Vol. 50, 2011, pp. 831–842.
[31] Liao SJ. On the relationship between the homotopy analysis method and Euler transform, *Communications in Nonlinear Science and Numerical Simulation,* Vol. 14, 2010, pp. 1421-1431.